High-Precision Proton-Proton Bremsstrahlung Measurements below the Pion-Production Threshold

H. Huisman, J. C. S. Bacelar, M. J. van Goethem, M. N. Harakeh, M. Hoefman, N. Kalantar-Nayestanaki, H. Löhner, J. G. Messchendorp, R. W. Ostendorf, S. Schadmand,* O. Scholten, R. G. E. Timmermans, R. Turrisi,† M. Volkerts, and H. W. Wilschut

Kernfysisch Versneller Instituut, Zernikelaan 25, 9747 AA Groningen, The Netherlands

R. S. Simon

Gesellschaft für Schwerionenforschung, Planckstraße 1, D-64291 Darmstadt, Germany

A. Kugler and V. Wagner

Nuclear Physics Institute, 250 86 Řež u Prahy, Czech Republic

(Received 10 March 1999)

An exclusive proton-proton bremsstrahlung measurement has been performed with polarized protons of 190 MeV. Absolute cross sections and analyzing powers have been measured with unprecedented accuracy in a large part of the phase space. The data are compared with state-of-the-art theoretical calculations including higher-order off-shell effects, like the Δ isobar and meson-exchange currents. Surprisingly, the calculations are unable to describe the data in detail.

PACS numbers: 13.75.Cs, 25.10.+s, 25.20.Lj

Nucleon-nucleon bremsstrahlung is the most fundamental reaction with which one can study off-shell effects in the nucleon-nucleon (*NN*) interaction. In 1958 Low proved the soft-photon theorem, which states that in a series expansion in the photon momentum, the first two terms of the scattering amplitude can be expressed exactly in terms of the elastic amplitude for the same system [1,2]. Current potential models describe the elastic data very accurately and therefore also soft-photon production. To test the off-shell behavior of the potentials, one has to go beyond the validity regime of the Low expansion and thus measure high-energy bremsstrahlung.

In the description of hard-photon production, the inclusion of the full dynamics of the intermediate off-shell nucleons is crucial. It has been a long-standing hope that the bremsstrahlung process will be able to discriminate between the different potential models. However, the predictions using different realistic *NN* potentials do not differ significantly [3]. The existing hard-photon data, though not precise, were not completely described by the models. This led to attempts to investigate the sensitivity of the observables to higher-order off-shell effects. The effects considered include negative-energy states [4], the virtual Δ isobar and the magnetic meson-exchange currents (MEC) [5–9], and the explicit off-shell dependence of the electromagnetic $NN\gamma$ vertex [10,11]. For the kinematics presented in this Letter, the inclusion of the virtual Δ isobar and MEC contribute up to 8% to the cross section [9]. For the first time, we present in this Letter high-accuracy results on proton-proton bremsstrahlung ($pp\gamma$) required to distinguish the effects just discussed at energies below the pion-production threshold where the interpretation of the results are relatively simple. The aforementioned issues are relevant not only for bremsstrahlung but also in other subfields such as Compton scattering and meson production, spanning a large part of nuclear physics from the *NN* interaction to nuclear matter.

The experimental efforts in $pp\gamma$ have always been hampered by the dominant elastic-scattering background. It was not until the 1980's that the first high-luminosity experiment for small outgoing proton angles was performed at TRIUMF at 280 MeV incident energy [12]. Another experiment, at a beam energy of 294 MeV, has been performed at IUCF [13], but comparison with theory is difficult due to the integration of the data over parts of the phase space. Recently an experiment has been performed at RCNP, Osaka, at a higher incident energy of 389 MeV [14]. This experiment aims explicitly at Δ production in the bremsstrahlung process, allowing examination of the models in a different regime than at the lower energies. Therefore, the information obtained from these measurements is complementary to that from the measurements done at lower energies. Presently, results of other $pp\gamma$ experiments, at beam energies around the pion production threshold, performed in Uppsala [15] and Jülich [16] with lower luminosities, are also becoming available. In this Letter, we report on the $pp\gamma$ cross sections and analyzing powers at a beam energy of 190 MeV measured with very high accuracy. In principle, this allows for a detailed test of extensive model calculations, including higher-order effects, such as the Δ isobar and meson-exchange currents. More importantly, the full dynamics of the intermediate nucleons during a very hard bremsstrahlung process can be investigated. Furthermore, a measurement of virtual bremsstrahlung in *pp* scattering allows for determination of the longitudinal response functions, which are not accessible in real bremsstrahlung [17].

0031-9007/99/83(20)/4017(4)$15.00

In Fig. 1 a schematic top view of the complete setup is shown. The 190 MeV polarized-proton beam of the superconducting cyclotron AGOR was used to bombard a liquid-hydrogen target [18]. To probe intermediate states far off the mass shell, one needs to measure the cross section for emission of high-energy photons. This requires the detection of both protons at small laboratory angles. To this end, we designed and built the Small-Angle Large-Acceptance Detector, SALAD [19]. This device provides azimuthally symmetric acceptance and detects particles between 6° and 26° and proton energies between 15 and 135 MeV with a resolution of better than 10%. The polar angular resolution is 0.5°. The large solid angle (≈400 msr) is mandated by the very small cross section for the $pp\gamma$ process. The angles of the scattered particles are determined with two multiwire proportional chambers with a central hole [20], to allow free beam passage. Furthermore, two layers of plastic scintillators are used. The first layer will stop protons with energies up to 135 MeV. Protons with a higher energy at these angles are due to elastic scattering. They will punch through the first layer and penetrate into the second. A special trigger system was designed [21] to reject these protons. The bremsstrahlung photons were detected with the Two-Arm Photon Spectrometer, TAPS [22]. TAPS consists of approximately 400 BaF_2 crystals, which were mounted in a large hexagon-shaped structure, surrounding the beam pipe. This setup has a polar angular range of 125°–170° and a complete azimuthal coverage. The angular resolution is about 6°. The cylindrical symmetry is essential in integrating the data over the whole azimuthal range to obtain a high statistical accuracy. TAPS covered more than 20% of the full 4π solid angle.

Because of the high rate of ≈12 MHz of elastic scattering, only 2% of the collected events are $pp\gamma$ events,

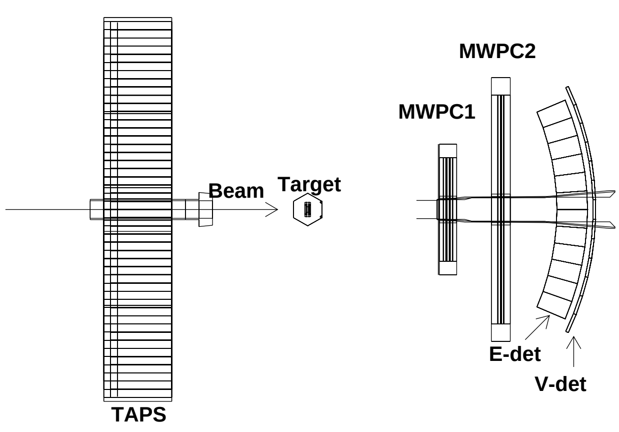

FIG. 1. Schematic top view of the SALAD and TAPS detectors in the present setup. The SALAD detector was used for the detection of protons. The photons were detected with the TAPS detector, which was mounted at backward angles in the shape of a large hexagon. The complete setup is equipped with a central hole to allow beam passage. See text for more details.

the rest being events that could not be eliminated by the trigger. The $pp\gamma$ events are extracted in an off-line analysis. The photons detected in TAPS are discriminated from massive particles by time of flight. For a further reduction of the background, the overdetermined kinematics of the $pp\gamma$ events is used. The 3-body final state has nine kinematic variables of which only five are free because of energy and momentum conservation. All nine variables are measured, providing four redundant variables. As the scattering angles are the best determined variables, the polar and azimuthal angles of the two protons and the polar angle of the photon are used to reconstruct the other four variables. Since the reconstruction of background events will in general produce forbidden momenta, for example, a negative energy for one of the particles, kinematic reconstruction provides a major reduction of the background. The accumulated effect of time cuts, kinematical reconstruction, and using only one of the redundant variables reduces the background to a level of less than 1%.

Several corrections have to be made to obtain absolute cross sections. The first corrections are due to the cuts made to select clean data and to the geometrical acceptance. These efficiencies were investigated by means of Monte Carlo simulations [23] and are always found to be larger than 92%. The second correction is due to the detection efficiency of the wire chambers, which was extracted from the data [20] and was typically 93%. Thirdly, the efficiency of the trigger to identify $pp\gamma$ candidates was investigated [21], and was typically 91%. Finally, the luminosity and beam polarization were determined by using the recorded downscaled elastic-scattering events. The measured angular distribution of pp elastic scattering was fitted to two phase-shift analyses, from VPI [24] and Nijmegen [25], with only the normalization magnitude as a free parameter. The fitted normalization has a statistical error of less than 1%. This normalization is used to obtain absolute cross sections. The beam polarization was extracted by fitting the polar angular distribution of left-right asymmetries to the analyzing powers of the same two pp phase-shift analyses. Its value is typically 0.65 with an accuracy of 0.01.

The complete data set consists of about 4.5 million bremsstrahlung events. For brevity, we present in this Letter only a small fraction of the covered phase space, comprising about 100 000 events. These are, however, representative of the larger data set and the final conclusions drawn in this paper apply to the whole data set.

For the kinematics we have used the conventions of Drechsel and Maximon [26]. In Fig. 2 the measured cross sections and analyzing powers are shown as a function of one of the proton angles. The errors indicated in the figure are statistical only. In the left panel, the angle of proton 1 is varied, while the angle of proton 2 is fixed at 16°. Proton 1 is defined as the proton which lies on the same side of the beam as the photon. The photon

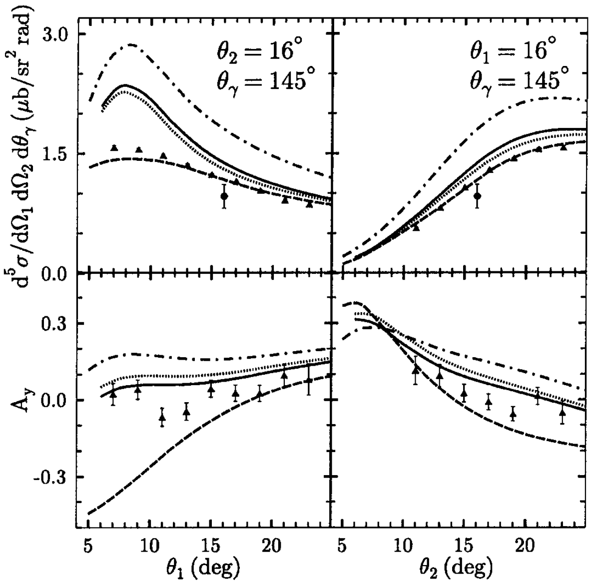

FIG. 2. Coplanar $pp\gamma$ cross sections and analyzing powers measured at 190 MeV incident energy at $\theta_\gamma = 145°$. The data point shown as the dot with error bar is from a measurement at 200 MeV of Ref. [28]. The dash–double-dotted curve is the microscopic calculation of Ref. [4]. The solid curve includes in addition MEC and the Δ isobar [9]. The dashed curve is a SPA calculation [29] and the dash-dotted curve is a microscopic calculation by Eden and Gari [8,33].

scattering angle is fixed at 145°, with a bin size of 10° (140°–150°). In the right panel, the angle of proton 1 is fixed at 16° and the angle of proton 2 is varied. The bin size in proton angles is 2°. The bin size in noncoplanarity (see Ref. [26]) is 5°, with its central value at 2.5°. For all practical purposes the presented data set can be considered coplanar [27].

The error in the determination of the overall normalization of the bremsstrahlung cross section is due to several different sources: the error in the measurement of the elastic cross section, the error in the trigger efficiency, and the error in the corrections made with the Monte Carlo simulations. Adding these errors in quadrature results in a 5% error in the overall normalization. Furthermore, the relative systematic error (point-to-point) on the data is 2%, due to uncertainties in determining the wire-chamber efficiencies. The errors in the analyzing powers are determined by statistics only. In Tables I and II the data are listed with both statistical and systematic errors. The cross sections are consistent with a prior measurement at 200 MeV incident energy [28] as shown by the data point (dot with error bar in Fig. 2) at $\theta_\gamma = 142.5°$.

Also shown in Fig. 2 are four different theoretical predictions. The dashed curve shows the result of a soft-photon amplitude (SPA) calculation [29], which uses the elastic-scattering phase shifts of Ref. [30] as input. This SPA calculation is relativistic and gauge invariant and has been inspired by the soft-photon theorem [1,2], but also contains higher-order terms which partly mimic the off-shell behavior of the one-boson exchange *NN* interaction [29]. However, no detailed information on the underlying reaction dynamics can be obtained with SPA's. The dash–double-dotted curve is the result of a fully relativistic microscopic-model calculation by Martinus *et al.* [4] based on the Fleischer-Tjon *NN* potential [31]. It incorporates the off-shell dynamics of the intermediate nucleons and rescattering contributions. The solid curve is the result of a calculation by the same group and contains in addition the MEC currents and the virtual Δ isobar [9]. Negative-energy states do not contribute significantly at 190 MeV incident energy. One can see from Fig. 2 that the cross sections are in good agreement with the SPA but not with the more sophisticated microscopic model. The analyzing power is described neither by the SPA nor by the calculations of Martinus *et al.* [4,9]. Part of the discrepancy with this microscopic model resides in the fact that the *NN* potential of Ref. [31] does not provide a good fit to the present-day *NN* database. A preliminary study suggests that with better *NN* phase shifts the agreement of the microscopic model with the cross sections reported here improves. However, the discrepancy with the data is too large to be explained by this effect. In short, the discrepancy of our data with the microscopic-model calculations indicates that an explicit treatment of additional higher-order effects is still needed, or that the problem resides in the approximations made in modeling the off-shell *NN*

TABLE I. Measured $pp\gamma$ cross sections and analyzing powers at 190 MeV incident energy. The kinematics are coplanar, $\theta_\gamma = 145°$ and $\theta_2 = 16°$. There is a 5% systematic error in the overall normalization in the cross-section data, not shown in the table. The errors in parentheses reflect the point-to-point systematic error.

θ_1 [deg]	Cross section [μb/sr^{2}rad]	A_y
7	1.575 ± 0.023 (0.031)	0.022 ± 0.043
9	1.548 ± 0.020 (0.031)	0.040 ± 0.038
11	1.475 ± 0.017 (0.030)	−0.068 ± 0.025
13	1.352 ± 0.015 (0.027)	−0.046 ± 0.034
15	1.122 ± 0.014 (0.022)	0.043 ± 0.033
17	1.148 ± 0.012 (0.023)	0.026 ± 0.032
19	1.034 ± 0.011 (0.021)	0.025 ± 0.032
21	0.911 ± 0.014 (0.018)	0.096 ± 0.044
23	0.858 ± 0.018 (0.017)	0.079 ± 0.061

TABLE II. Same as Table I, except for $\theta_1 = 16°$.

θ_2 [deg]	Cross section [μb/sr^{2}rad]	A_y
11	0.564 ± 0.011 (0.011)	0.115 ± 0.055
13	0.818 ± 0.012 (0.016)	0.095 ± 0.043
15	1.075 ± 0.013 (0.022)	0.026 ± 0.035
17	1.294 ± 0.013 (0.026)	−0.009 ± 0.031
19	1.437 ± 0.013 (0.029)	−0.056 ± 0.028
21	1.551 ± 0.018 (0.031)	0.014 ± 0.034
23	1.568 ± 0.024 (0.031)	−0.051 ± 0.045

interaction. Other microscopic-model calculations yield similar results [3,32]. The one exception is a calculation by Eden and Gari [8,33] which produces systematically higher cross sections than other microscopic-model calculations. Their result is depicted by the dash-dotted curve in Fig. 2. The reasons for the disagreement between the calculations by Eden and Gari and the other microscopic calculations are not yet clear.

In summary, a high-precision measurement of proton-proton bremsstrahlung cross sections and analyzing powers has been performed below the pion-production threshold at an incident energy of 190 MeV. Both protons were measured at small forward angles in coincidence with the photon at backward angles. The combined statistical and systematic error in the measurements is superior to that in any prior measurement of this process, allowing, for the first time, a detailed comparison between the data and theoretical models. Calculations for the present kinematics have been performed with a relativistic and gauge-invariant SPA and with two microscopic models. Surprisingly, the SPA of Ref. [29] with its specific way of calculating the amplitudes describes the measured cross sections better than the microscopic models. The analyzing powers are, on the other hand, better described by the microscopic calculations of Ref. [9]. Since the microscopic models disagree both in magnitude and shape with the cross sections and analyzing powers presented in this Letter, we conclude that to this date no high-quality *NN* model calculation consistent with the data exists. It is remarkable that for such a simple, yet fundamental, system we still lack a good understanding of the underlying dynamics.

The authors would like to acknowledge the support by the TAPS collaboration in bringing the Two-Arm Photon Spectrometer into operation at KVI. They also express their appreciation for the tireless efforts of the cyclotron and ion-source groups in delivering the high-quality beam used in these measurements. The authors thank J. A. Eden for making his computer code available for the calculation of $NN\gamma$ observables. S. Kondratyuk and G. H. Martinus are thanked for providing the results of their calculations. The help of M. C. M. Rentmeester in providing the normalization of the elastic pp data is appreciated. This work is part of the research program of the "Stichting voor Fundamenteel Onderzoek der Materie" (FOM) with financial support from the "Nederlandse Organisatie voor Wetenschappelijk Onderzoek" (NWO).

*Present address: Universität Gieβen, Heinrich-Buff-Ring 16, D-35392 Gieβen, Germany.

†Present address: GANIL, BP no. 5027, F-14021 Caen Cedex, France.

[1] F. E. Low, Phys. Rev. **110**, 974 (1958).
[2] E. M. Nyman, Phys. Lett. **25B**, 135 (1967); Phys. Rev. **170**, 1628 (1968).
[3] V. Herrmann and K. Nakayama, Phys. Rev. C **45**, 1450 (1992).
[4] G. H. Martinus, O. Scholten, and J. A. Tjon, Phys. Rev. C **56**, 2945 (1997).
[5] F. de Jong *et al.*, Phys. Lett. B **333**, 1 (1994); F. de Jong, K. Nakayama, and T. S. H. Lee, Phys. Rev. C **51**, 2334 (1995).
[6] F. de Jong and K. Nakayama, Phys. Rev. C **52**, 2377 (1995).
[7] M. Jetter and H. W. Fearing, Phys. Rev. C **51**, 1666 (1995).
[8] J. A. Eden and M. F. Gari, Phys. Rev. C **53**, 1102 (1996).
[9] G. H. Martinus, O. Scholten, and J. A. Tjon, Phys. Lett. B **402**, 7 (1997); Phys. Rev. C **58**, 686 (1998).
[10] Yi Li, M. K. Liou, and W. M. Schreiber, Phys. Rev. C **57**, 507 (1998).
[11] S. Kondratyuk, G. H. Martinus, and O. Scholten, Phys. Lett. B **418**, 20 (1998).
[12] K. Michaelian *et al.*, Phys. Rev. D **41**, 2689 (1990).
[13] B. von Przewoski *et al.*, Phys. Rev. C **45**, 2001 (1992).
[14] K. Yasuda *et al.*, Phys. Rev. Lett. **82**, 4775 (1999).
[15] J. Złomańczuk, A. Johansson, and the WASA-PROMICE Collaboration, Nucl. Phys. **A631**, 622c (1998).
[16] R. Bilger *et al.*, Phys. Lett. B **429**, 195 (1998).
[17] J. G. Messchendorp *et al.*, Phys. Rev. Lett. **82**, 2649 (1999); **83**, 2530 (1999).
[18] N. Kalantar-Nayestanaki, J. Mulder, and J. Zijlstra, Nucl. Instrum. Methods Phys. Res., Sect. A **417**, 215 (1998).
[19] N. Kalantar-Nayestanaki, Nucl. Phys. **A631**, 242c (1998); N. Kalantar-Nayestanaki *et al.*, Nucl. Instrum. Methods Phys. Res., Sect. A (to be published).
[20] M. Volkerts *et al.*, Nucl. Instrum. Methods Phys. Res., Sect. A **428**, 432 (1999).
[21] S. Schadmand *et al.*, Nucl. Instrum. Methods Phys. Res., Sect. A **423**, 174 (1999).
[22] A. R. Gabler *et al.*, Nucl. Instrum. Methods Phys. Res., Sect. A **346**, 168 (1994).
[23] *GEANT* Application Software Group, CERN Program Library Long Writeup W 5013.
[24] R. A. Arndt *et al.*, Phys. Rev. C **56**, 3005 (1997).
[25] M. C. M. Rentmeester *et al.*, Phys. Rev. Lett. **82**, 4992 (1999).
[26] D. Drechsel and L. C. Maximon, Ann. Phys. (N.Y.) **49**, 403 (1968).
[27] Yi Li, M. K. Liou, R. Timmermans, and B. F. Gibson, Phys. Rev. C **58**, R1880 (1998).
[28] J. G. Rogers *et al.*, Phys. Rev. C **22**, 2512 (1980).
[29] M. K. Liou, R. G. E. Timmermans, and B. F. Gibson, Phys. Rev. C **54**, 1574 (1996); Phys. Lett. B **345**, 372 (1995).
[30] J. R. Bergervoet *et al.*, Phys. Rev. C **41**, 1435 (1990).
[31] J. Fleischer and J. Tjon, Nucl. Phys. **A84**, 375 (1974); Phys. Rev. D **15**, 2537 (1977); **21**, 87 (1980).
[32] K. Nakayama (private communication).
[33] J. A. Eden (private communication).